

Recent Results from the SAFIR Project¹

M. Sánchez-Portal^{1,2}, M. Castillo-Fraile^{1,2}, C. Ramos Almeida³, P. Esquej^{4,5}, A. Alonso-Herrero⁵, A. M. Pérez García³, J. Acosta-Pulido³, B. Altieri¹, A. Bongiovanni³, J. M. Castro Cerón¹, J. Cepa³, D. Coia¹, L. Conversi¹, J. Fritz⁶, J. I. González-Serrano⁵, E. Hatziminaoglou⁷, M. Pović⁸, J. M. Rodríguez Espinosa³, I. Valtchanov¹

¹European Space Astronomy Centre (ESAC)/ESA, Madrid, Spain

²ISDEFE, Madrid, Spain

³Instituto de Astrofísica de Canarias, La Laguna, Tenerife, Spain

⁴Centro de Astrobiología, INTA-CSIC, Madrid, Spain

⁵Instituto de Física de Cantabria, CSIC-UC, Santander, Spain

⁶Sterrenkundig Observatorium, Universiteit Gent, Belgium

⁷European Southern Observatory, Garching bei München, Germany

⁸Instituto de Astrofísica de Andalucía, Granada, Spain

Corresponding author: miguel.sanchez@sciops.esa.int

Abstract

The “Seyfert and star formation Activity in the Far-Infrared” (SAFIR) project is aimed at studying the physical nature of the nuclear IR emission and star formation properties of a small sample of nearby Seyfert galaxies observed with the PACS and SPIRE instruments on board the *Herschel* space observatory. In this paper, we review the achieved results, that reveal the importance of the far-IR range to improve the quality and reliability of the estimates of basic AGN torus parameters, and describe some preliminary outcome from the on-going work on the dust properties of resolved AGN host galaxies.

Keywords: AGN - Seyfert - SED - IR.

1 Introduction

Coeval AGN and starburst phenomena can be assessed by means of the analysis of dust in the infrared (IR) domain. In this range, in particular in the mid-IR (MIR) and far-IR (FIR), dust contributes to most of the thermal emission. The unified model considers a central AGN engine and a broad-line region (BLR) obscured by a thick dust torus. The dust grains re-radiate in the IR the absorbed UV/optical photons. As it has been well characterised by existing facilities (eg. *Spitzer*, T-ReCS), the dusty torus emission peaks in the MIR (7–30 μm) and it extends to the FIR, where the contribution related to the star formation (SF) becomes dominant. Thus, agreeing to [8], the SED of Seyfert galaxies in the MIR and FIR range can be solely explained by the dust thermal re-radiation of higher energy photons. Therefore, dust thermal emission should be made-up of three different contributions: (a) warm dust heated by

the AGN (120–170 K); (b) cold dust heated by the star formation (40–70 K, and (c) very cold dust heated by the general interstellar radiation field (15–25 K). Until now it has been poorly constrained due to the limited spatial resolution and spectral coverage of the existing facilities. The *Herschel* observatory [5] provides new performances and capabilities to study the emission of nearby galaxies in FIR and sub-mm regions: the PACS [9] photometer allows to image in the 70, 100 and 160 μm with unprecedented spatial resolution (5.5 arcsec at 70 μm) and the SPIRE [3] photometer permits to image in the 250, 350, 500 μm bands, a formerly unexplored region, at a relatively high spatial resolution. These instruments provide, on the one hand the characterisation of the AGN SED minimizing the contamination by the host galaxy (PACS) and on the other, the assessment of the cold and very cold dust components (SPIRE) both across the host galaxy and the nuclear and circum-nuclear regions. PACS and SPIRE data can

¹*Herschel* is an ESA space observatory with science instruments provided by European-led Principal Investigator consortia and with important participation from NASA.

be used to fit SEDs sampling both the emission peak and the Rayleigh-Jeans tail of the thermal emission of the cold and very cold dust components. The fitted SEDs can be used to derive dust masses and temperatures and the star formation rate (SFR). The relatively high spatial resolution of these instruments makes possible to map the different emission regions (e.g. nucleus, arms, inter-arm region). In this context, two foci of interest drive the SAFIR study: (a) The dusty torus: current models consider either smooth or clumpy dust distributions. Any AGN IR model should consider three constituents when applied to describe the actual SED of Seyfert galaxies: AGN, starburst and host galaxy. The starburst contribution can be constrained by the use of FIR data. In addition, both the torus and starburst emission overlap smoothly in the FIR. Therefore, the use of FIR data with high spatial resolution and wide spectral range coverage is fundamental to discriminate the modelled torus characteristics. (b) The nuclear activity and star formation coexistence: the interrelationship between accretion onto massive black holes and the star formation is a topic fundamental to understand the formation and evolution of galaxies. FIR data from *Herschel* PACS and SPIRE allow to characterise and map the dust distribution and temperature and the star formation activity across galaxies hosting AGNs. It can contribute to constraint the current AGN formation and evolution models.

2 Sample of Galaxies and Technical Implementation

The SAFIR collection of nearby galaxies is constituted by 18 Seyfert galaxies sampled to represent different nuclear classes (Seyfert 1.x & Seyfert 2). Only objects with available high-resolution MIR data (ground-based or *Spitzer*) were selected. In addition, all the objects have available optical, NIR, X-radio and radio data. This allows to construct a complete multi-wavelength SED for all the objects of the sample. Ten galaxies of the sample are barred spiral/lenticulars and five are peculiar/interacting systems. Four objects are confirmed Luminous or Ultra-luminous IR galaxies (LIRG/ULIRG). The observations were performed in the PACS and SPIRE scan map modes adjusting the mapped areas to fit the host galaxy and a background region within the surveyed area. The achieved 1σ sensitivities were approximately, 3.6, 3.9 and 3.9 mJy/beam for PACS at 70, 100 and 160 μm and 5.5, 7.6 and 6.4 mJy/beam for SPIRE at 250, 350 and 500 μm . With these sensitivities it was possible to map both the nuclear and circum-nuclear regions and also large areas within the galaxy disks.

3 Results

This section presents some already published results from the SAFIR project [10, 2, 1] for three objects of the sample.

3.1 NGC 3081

This galaxy was studied in the context of the SAFIR project combining PACS/SPIRE data with ground-based high-resolution NIR/MIR data [10]. This object is an early-type barred spiral ((R)SAB0/a(r)). It comprises a series of well defined nested star-forming annular-like features: nuclear (r1, 2.3 kpc), inner (r2, 11 kpc) and outer (26.9 kpc) rings. The inner ring (r2) is evidently resolved in the images up to 250 μm . The nuclear SED was fitted combining unresolved FIR fluxes ($r \leq 1.7$ kpc) together with integrated NIR and MIR data. A clumpy model was applied to simulate the nuclear torus emission [4] to assess how the torus parameters have to be modified, in particular the torus size to account for the FIR emission. As a result, it was obtained that the torus outer radius must be notably increased: $R_o = 4_{-1}^{+2}$ pc vs. $R_o = 0.7 \pm 0.3$ pc obtained using only NIR and MIR data [11]. Also the radial distribution of clouds (defined by the power-law index of the radial density profile q) flattens when the FIR data are included in the simulation: ($q = 0.2$ vs $q = 2.3$). Other model parameters (width of the angular distribution, inclination angle, optical depth, number of clouds) are in agreement with those obtained without FIR data. At larger scales ($1.7 \text{ kpc} \leq r \leq 5.4 \text{ kpc}$), the FIR emission is well characterised by cold dust thermal emission at $T = 28 \pm 1$ K (assuming a grey blackbody with emissivity $\beta = 2$) likely heated by young stars in r1. The FIR emission of the outer part of the galaxy can be reproduced with very cold dust ($T = 19 \pm 3$ K) heated by the interstellar radiation field.

3.2 Mrk 938

This galaxy contains a Seyfert 2 AGN and presents a significant starburst activity. This object is a morphologically peculiar galaxy that has been proposed to be the remnant of a gas-rich merging of two unequal mass galaxies [12]. It is classified as LIRG due to its large IR luminosity. A multi-wavelength study was performed for this object combining X-ray, NIR, MIR and PACS/SPIRE FIR data in the context of the SAFIR project [2] in order to characterise the origin and nature of its strong emission in the IR range. The AGN bolometric contribution to the MIR and the total IR luminosity is small [$L_{bol}(\text{AGN})/L_{IR} \sim 0.02$] as observed in the component decomposition of the MIR *Spitzer*/IRS spectrum, which is in agreement with previous estimations. The MIPS 24 μm and PACS 70 μm images indi-

cate that the major part of the star formation activity is concentrated in a compact obscured region of ≤ 2 kpc. FIR data have been used to constraint the cold dust emission with unprecedented accuracy. In order to derive the dust properties, the integrated IR SED has been fitted. It has been found that the MIR to FIR spectrum can be properly modelled by a two-component SED: two modified blackbodies with fixed emissivity ($\beta=2$) and temperatures $T_w=67$ K and $T_c=35$ K for the warm and cold dust components, respectively. In addition, a single blackbody component SED was fitted to the FIR-only spectrum with a modified blackbody of $\beta=2$ and $T=36.5$ K. This value has been used along with the SPIRE flux at $250\ \mu\text{m}$ to derive the dust mass using Eq. 2 considering an absorption coefficient $\kappa_{250\mu\text{m}}=4.99\ \text{cm}^2\text{g}^{-1}$. The value obtained for the dust mass, $M_{\text{dust}}=3\times 10^7 M_{\odot}$, is consistent with those derived for local ULIRGs and other IR-bright galaxies.

3.3 NGC 1365

NGC 1365 (Fig. 1, left) is a supergiant barred spiral galaxy (SB(s)b). It is a nearby (18.6 Mpc) LIRG harboring a Seyfert 1.5 type nucleus. The inner Lindblad resonance (ILR) region of the galaxy contains a powerful nuclear starburst ring with an approximate diameter of 2 kpc. We have probed the nuclear and circum-nuclear activity of this galaxy in the IR [1]. The strong star formation activity in the ring is resolved by the *Herschel*/PACS imaging data that shows some substructures (super star clusters), as well as by the *Spitzer* $24\ \mu\text{m}$ continuum emission, [Ne II] $12.81\ \mu\text{m}$ line emission, and 6.2 and $11.3\ \mu\text{m}$ PAH emission. The active galactic nucleus (AGN) is the brightest source in the central region up to $\lambda\sim 24\ \mu\text{m}$, but it becomes increasingly fainter in the FIR when compared to the emission originating in the IR clusters located in the ring. We modelled the AGN unresolved IR emission with a clumpy torus model and estimated that the AGN contributes only in a small fraction ($\sim 5\%$) of the IR emission produced in the inner ~ 5 kpc. The estimated torus size is ~ 5 pc. We fitted the non-AGN $24\text{--}500\ \mu\text{m}$ SED of the region within the ILR and found that the dust temperature and mass are similar to those of other nuclear and circum-nuclear starburst regions. Finally, the comparison of the IR-derived SFR with that obtained from H α observations indicates that $\sim 85\%$ of the on-going star formation within the ILR is taking place in dust-obscured regions.

4 Dust Properties of Resolved AGN Host Galaxies

A study of the dust properties of spatially well-resolved AGN hosts has been started (Sánchez-Portal, Castillo-Fraile et al. in preparation). Within the SAFIR sam-

ple, four galaxies (NGC 1365, NGC 4258, NGC 1566 and NGC 5728) have an apparent size large enough to allow a detailed analysis of the spatial dust properties, notably its temperature and mass that can be directly compared with the star formation characteristics. For these objects, the spatial resolution of the observations is being exploited to produce maps of the dust mass, temperature, and SFR. In this section some examples of the activities currently on-going are shown.

Assuming an optically thin emission, the flux density can be expressed as $f_{\nu}\propto\nu^{\beta}B(\nu,T_{\text{dust}})$ where β is the dust emissivity. As already stated, several dust components with different temperature should be generally considered, so the flux density can be expressed as:

$$f_{\nu}(\lambda)=\sum_{i=1}^n\frac{N_i}{\lambda^{\beta+3}(e^{hc/\lambda kT_i}-1)}\quad (1)$$

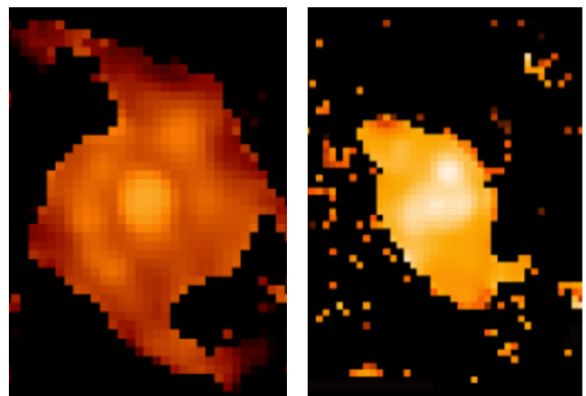


Figure 1: Temperature maps of NGC 1365 (left) and NGC 1566 (right). Average temperatures range from $\sim 17\text{--}18$ K in the inter-arm regions to $T\sim 23\text{--}24$ K in the bright spots within the spiral arms. The highest average dust temperatures are observed in the central region of NGC 1365 with $T\sim 26$ K.

where N_i are the normalization constants and T_i are the temperatures of the different components. The procedure devised to generate temperature maps includes the following steps: after a standard reduction procedure (see [1] for a description), the PACS 70, 100 and $160\ \mu\text{m}$ and SPIRE 250 and $350\ \mu\text{m}$ maps have been convolved to the resolution of the SPIRE $500\ \mu\text{m}$ images and resampled to the largest pixel size (that of the SPIRE $500\ \mu\text{m}$ maps, set to 14 arcsec). The images have been spatially registered and used as input to an IDL procedure that performs a least-squares fit to either one or two dust components ($n=1$ or 2) at each pixel in order to cope with the cold or/and very cold dust components.

In the maps shown in Fig. 1 we have used a single temperature component with a fixed emissivity $\beta=2$ to create the temperature maps of NGC 1365 (top) and

NGC 1566 (bottom). The latter is a bright (LC II-III), nearby (11.83 Mpc) SAB(s)bc spiral galaxy harboring a Seyfert type 1.5 nucleus.

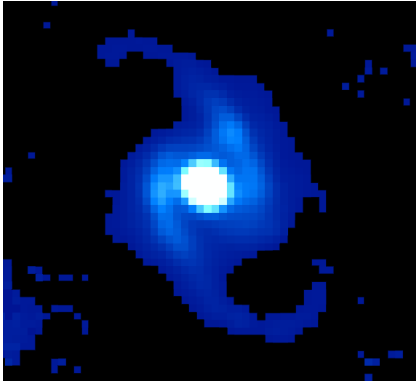


Figure 2: SFR map of NGC 1365, obtained from the grey body IR luminosity integrated between 8 and 1000 μm .

The temperature maps generated closely follow the topology of the star formation regions, with the highest temperatures corresponding to areas of high SF activity, as observed by comparison with the morphology of 70 μm and optical H α images. In fact, we have created SFR maps by integrating the grey body SED at the best-fit temperature and applying standard scaling relations [7]. In Fig. 2 we show the SFR map of NGC 1365. There is an excellent agreement with the structures revealed by the dust temperature map and the SFR density. In agreement with [1], it is observed that the most intense star formation is taking place in the circum-nuclear region (within the ILR). Outstanding formation rate is also taking place in the spiral arms.

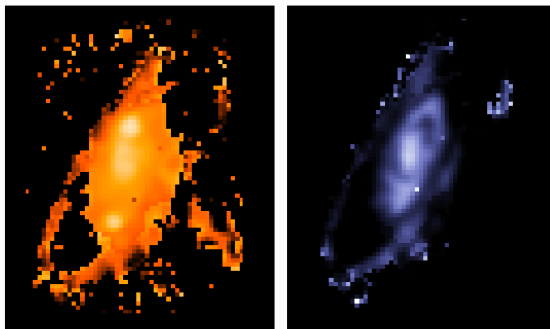


Figure 3: NGC 4258 Temperature (left) and dust mass (right).

The spatial distribution of dust mass (projected dust density) can be obtained from the temperature maps, using the expression:

$$M_{dust} = \frac{D_L^2 f_\nu}{\kappa_\nu B_\nu(T_{dust})} \quad (2)$$

adapted from [6], where D_L is the luminosity distance and f_ν is extracted from the SPIRE flux

map at 250 μm assuming an absorption coefficient $\kappa_{250\mu\text{m}} = 4.99 \text{ cm}^2 \text{ g}^{-1}$. In Fig. 3 we present the dust temperature and mass maps of NGC 4258, a bright (LC II-III), nearby (7.44 Mpc) SAB(s)bc spiral galaxy hosting a LINER/Seyfert 1.9 nucleus. The pixel scale is 0.36 Kpc $^{-2}$.

5 Conclusions

The high spatial resolution *Herschel* PACS & SPIRE observations are demonstrating the importance of the FIR to improve the quality and reliability of the AGN torus fits. Parameters as important as the torus radius and cloud radial distribution have a strong dependency of this spectral range. Moreover, the FIR data are crucial to characterise the starburst contribution and to constrain the dust properties. The quality of the *Herschel* data is allowing us to study the spatial distribution of dust within the galaxies, thus permitting to characterize the variation of dust properties (temperature, dust mass) and SFR with the nuclear distance.

Acknowledgments

We would like to acknowledge the *Herschel* Project Scientist, Göran Pilbratt, for making possible the implementation of this project kindly providing the required guaranteed time from the PS budget.

References

- [1] Alonso-Herrero, A., Sánchez-Portal, M., Ramos Almeida, C., et al. 2012, MNRAS, 425, 311 doi:10.1111/j.1365-2966.2012.21464.x
- [2] Esquej, P., Alonso-Herrero, A., Pérez-García, A. M., et al. 2012, MNRAS, 423, 185 doi:10.1111/j.1365-2966.2012.20779.x
- [3] Griffin, M.J., Abergel, A., Abreu, A. et al. 2010, A&A, 518, L3
- [4] Nenkova M. et al., 2008, ApJ, 685, 147 doi:10.1086/590482
- [5] Pilbratt, G.L., Riedinger, J.R., Passvogel, T. et al. 2010, A&A, 518, L1
- [6] Hildebrand R. H., 1983, Q. J. R. Astron. Soc., 24, 267
- [7] Kennicutt, Jr., R. C., ARAA, 1998, 36, 189 doi:10.1146/annurev.astro.36.1.189
- [8] Pérez García A. M., Rodríguez Espinosa J. M., 2001, ApJ, 557, 39 doi:10.1086/321675
- [9] Poglitsch, A., Waelkens, C., Geis, N. et al. 2010, A&A, 518, L2
- [10] Ramos Almeida, C., Sánchez-Portal, M., Pérez García, A. M., et al. 2011, MNRAS, 417, L46 doi:10.1111/j.1745-3933.2011.01117.x
- [11] Ramos Almeida C. et al., 2011, ApJ, 731, 92 doi:10.1088/0004-637X/731/2/92
- [12] Schweizer F., Seitzer P., 2007, AJ, 133, 2132